


Hydrogen Interactions with Defects in Materials

Astrid Pundt* and Stefan Wagner

DOI: 10.1002/cite.202300235

 This is an open access article under the terms of the Creative Commons Attribution-NonCommercial-NoDerivs License, which permits use and distribution in any medium, provided the original work is properly cited, the use is non-commercial and no modifications or adaptations are made.

This manuscript summarizes basic properties of hydrogen in materials, mainly metals, and resulting consequences for the materials properties, including recent developments. It emphasises to introduce into the field of hydrogen in metals in a focused manner. It addresses hydrogen solution in materials, hydride formation, hydrogen diffusion and permeation and the interaction of hydrogen with defects. The influence of hydrogen on the defect energies and consequences for the metal behaviour are addressed. Further, the influence of constraint conditions on the system properties is shortly discussed.

Keywords: Coatings, Embrittlement, Hydrogen, Permeation

Received: December 01, 2023; *accepted:* December 20, 2023

1 Introduction

Hydrogen as the smallest of all atoms is solved in the interstitial sites of a metal lattice. It migrates faster than all other elements, especially at low temperatures. There is a thermodynamic equilibrium condition between the outside gas pressure p_{H_2} and the concentration of hydrogen x_{H} in the material [1]. For metals, hydrogen solves as a single atom, resulting in Sieverts' law (see Sect. 3). The process of hydrogen uptake concerns different intermediate steps (Fig. 1) such as adsorption (2) and dissociative chemisorption (3) of the hydrogen gas molecule into single atoms at the material surface, absorption via sub-surface sites and diffusion (4) into the bulk material to defects (see Sect. 2). Fig. 1 illustrates these steps for a surface crack.

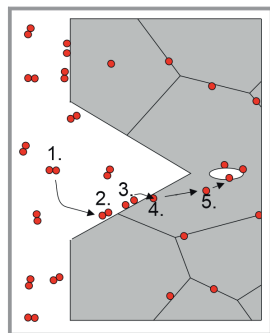


Figure 1. Hydrogen molecules approaching the crack tip via (1) H_2 -Gas transport, (2) H_2 molecule adsorption at the surface, (3) dissociative H-chemisorption, (4) H-absorption, (5) diffusion to a defect (6). The defect here is a pore. Based on the sketch of Vehoff et al. [2].

Hydrogen segregates in open-volume regions such as vacancies in the host lattice, at dislocations, at grain boundaries, interfaces and surfaces (see Sect. 5). Such defects are commonly present in the metal microstructure, depending on the production process. In additively manufactured metals or metals processed under large degrees of deformation, the density of defects can be high and controls the mechanical materials behaviour. Hydrogen segregating in these regions can change the local inter-atomic bonding and

hence further affect the mechanical properties. Even though the solubility of hydrogen in the host lattice might be small, locally high concentrations are reached at defects due to trapping effects. As hydrogen migrates fast in the metal (see Sect. 6), the traps commonly will be reached at reasonable time scales. Safety aspects are targeted throughout the paper, but not in a specific chapter.

Since in metals or metal alloys hydrogen is solved in interstitial lattice sites as an atom or ion, it shares its electron with the host lattice. In some metals and alloys, high hydrogen concentrations can be reached and new phases (hydrides) can occur (Sect. 4) next to the solid solution phase. Some of these hydrides may be used for hydrogen storage (FeTi or LaNi_5). For structural materials, the maximum hydrogen content should remain low. Some details of the different topics are outlined in the following chapter, by using Pd-H and Nb-H as general model systems.

2 Converting the H_2 Gas Molecule into H-Atoms

When the hydrogen gas molecule approaches the surface of a metal, it can adsorb by weak physisorption staying in the molecular configuration, or bind to the surface via chemisorption. [3, 4]. If this chemisorption dissociates the molecule, hydrogen can enter the metal lattice as atoms. For Pd(110), (111), and (100) surfaces, Conrad et al. [5] and Behm et al. [6] confirmed dissociative chemisorption. Hence, Pd but also Ni and some other metals are capable of

¹Prof. Dr. Astrid Pundt  <https://orcid.org/0000-0002-6665-6745> (astrid.pundt@kit.edu), ¹Dr. Stefan Wagner

¹Karlsruher Institut für Technologie (KIT), Institut für Angewandte Materialien-Werkstoffkunde (IAM-WK), KIT-Campus Süd, Kaiserstraße 12, 76131 Karlsruhe, Deutschland.

dissociating the H₂ gas molecule. As long as the dissociation of the H₂ gas molecule is hindered, hydrogen cannot enter the metal. Other sources for external atomic hydrogen can result from chemical reactions, when, e.g., water releases hydrogen ions or atoms during oxidation of a metal, or during pickling of metal surfaces. [7–9]

3 Low Hydrogen Concentrations in Ideal Solution: Sieverts' Law

For low concentrations in the solid solution of the metal, the hydrogen content x_{H} in interstitial sites of the bulk lattice often is found to scale with the square root of the pressure p_{H_2} . This dependency is expressed by Sieverts' law.

$$x_{\text{H}} = \text{const} \cdot \exp\left(\frac{\Delta S_{\alpha}}{R}\right) \exp\left(-\frac{\Delta H_{\alpha}}{RT}\right) \sqrt{\frac{p_{\text{H}_2}}{p_0}} = K_{0,i} \sqrt{\frac{p_{\text{H}_2}}{p_0}} \quad (1)$$

Values for the entropy of hydrogen solution ΔS_{α} and the enthalpy of hydrogen solution ΔH_{α} are listed by Fukai [1]. p_0 gives the reference pressure of 1 bar, and $R = 8.314 \text{ J mol}^{-1} \text{ K}^{-1}$ is the universal gas constant. Eq. (1) results from the thermodynamical equilibrium condition of balanced chemical potentials. In equilibrium, the chemical potential of the hydrogen in the gas phase $\mu_{\text{H}_2, \text{gas}}$ equals the chemical potential of hydrogen in the metal $\mu_{\text{H}, \text{M}}$. Considering that the gas phase molecules contain two hydrogen atoms, it is $1/2 \mu_{\text{H}_2, \text{gas}} = \mu_{\text{H}, \text{M}}$. This factor 1/2 converts into the square-root dependency of the pressure in Sieverts' law. For molecular solution of hydrogen, present for example in polymers, equation (1) would convert into a linear dependency of the pressure. We note that the chemical potential scales with the logarithm of the hydrogen gas pressure p_{H_2} in the gas phase, or of the concentration x_{H} in the solid phase.

The hydrogen solubility $K_{0,i}$ strongly depends on the kind of the metal as mainly expressed by the enthalpy of hydrogen solution ΔH_{α} , that differs for the different metals. On top of the H₂-molecule dissociation energy, it varies from $-90.7 \text{ kJ mol}^{-1}$ for Sc to $+106.1 \text{ kJ mol}^{-1}$ for W. (1) Very negative values mean a very strong bonding tendency of hydrogen in the solid solution of the metal.

The hydrogen solubility $K_{0,i}$ scales with the temperature T via an Arrhenius dependency and decreases with T increase. For the same external hydrogen gas pressure then the amount solved on interstitial lattice sites is reduced, for higher T .

4 Hydride Phases

For many metal-hydrogen systems, new phases can develop, which are called hydrides. They contain a larger content of hydrogen x_{H} than the solid solution phase and often possess new lattice structures. Because of the high hydrogen con-

centration, some hydrides can be used to store hydrogen in the corresponding lattice. The volumetric hydrogen density in metals is about 2.3 times higher than the hydrogen density in the cold liquid hydrogen phase [10]. However, the gravimetric density is given by the host metal. Hence, for mobile application, the host has to be as light as possible.

The hydride phases are electronically and elastically stabilized. This can be understood by considering the following arguments: The elastic strain energy of the free metal-hydrogen system can be reduced by positioning hydrogen atoms in the strain field of the metal lattice around another hydrogen atom, that has already been dissolved. This yields an attractive elastic H-H interaction energy. Thus, hydrogen atoms prefer to share their elastic strain fields and tend to localize in close vicinity of each other. For some metals, the electronic energy can be lowered by localizing hydrogen in close vicinity to each other by forming new low energy hybrid states of hydrogen and the host metal in the electronic density of states. If both energy contributions are large, hydride phases appear. Hydride formation enthalpies are collected by Fukai. [1] In Fukai's data collection they range from -113 kJ mol^{-1} for Y-YH₂ to $-10.6 \text{ kJ mol}^{-1}$ for Mn-MnH. When hydrides are considered for reversible hydrogen storage, hydrogen also has to be removed from the host lattice. Therefore, very stable or very weak hydrides are not suitable for storage applications. Target for practical storage applications is a formation enthalpy in the range of -15 to -24 kJ mol^{-1} , giving a dissociation pressure of 1–10 bar at 0–100 °C. [11] For structural materials, any hydride formation should be excluded under the conditions of operation.

Owing to modified electronic densities of states, hydride formation can be accompanied by a change in the bonding character, changing the metal to a semiconductor or even an insulator. [12] This changes the electrical resistivity from metallic conducting to insulating, and the optical properties from metallic reflective to transparent, respectively. [13, 14, 15] For some materials, the hydrogen diffusivity is reduced by orders of magnitude in the hydride.

5 Microstructural Contributions to Solubilities in the Low Concentration Regime

The hydrogen atom is always larger than the interstitial site (Fig. 2a) and thus locally leads to lattice expansion and an increase in the strain energy. For many metals, the lattice expansion $\Delta V/V$ scales linearly with the hydrogen concentration, for example it is $\Delta V/V = 0.174x_{\text{H}}$ for Nb-H and $\Delta V/V = 0.19x_{\text{H}}$ for Pd-H. [16] As sketched in Fig. 2, this yields a driving force for the hydrogen to solve in open volume defects. For Nb vacancies, about 4 hydrogen atoms were found to localize in one vacancy. [17] For Pd, for grain boundaries and some phase boundaries (d), Mütschele and Kirchheim reported on a H solubility between that of the α - and the α' -phase of the Pd-H system. [18, 19] For the dilatation field of edge dislocations in Pd (e), Maxelon et al. revealed a cylin-

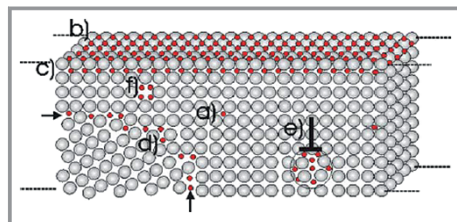


Figure 2. Hydrogen is located in interstitial lattice sites (a), and at open volume defects such as external surfaces and internal surfaces available in pores and internal cracks (b and c), grain boundaries or phase boundaries (d), in the dilatation field of dislocations (e) and in vacancies (f). With kind permission adapted from Ref. [24]

drical hydrogen rich region that increases with the hydrogen concentration up to 2 nm in diameter. [20,21] For external surfaces (b and c, surface and subsurface), Christmann [22] or Behm et al. [23] reported on 1 H/Pd or even higher local concentrations, depending on the type of surface phase. Internal surfaces available in pores and internal cracks might contain similar amounts of hydrogen.

The system total strain energy can be lowered by hydrogen ad- and absorption in these defects. Preferential hydrogen occupation in defect sites at low energies is called “trapping”, the related energy is called the “trap” binding energy. Hydrogen trapping in defects increases the total solubility in the metal. [19]

Trap binding energies can be measured by thermal desorption spectroscopy (TDS), using temperature ramping with different velocities. [25] At corresponding temperatures the trapped hydrogen desorbs from its trap, allowing to measure the trap binding energy. Alternatively, measurements of the electromotive force (EMF) can be used to determine the trap binding energies in the low concentration range. [26, 27, 28, 29]

The binding energies can be determined from the chemical potential μ_{H} considering the contributions of the major defects and the related energetic site distribution $Z(E)$. The hydrogen concentration can be gained by filling up the available energetic states with hydrogen atoms as a function of the chemical potential. As one interstitial site can just be occupied by one hydrogen atom and filled sites cannot be filled any more, the Fermi-Dirac statistics properly describes the filling process. [30]

$$x_{\text{H}}(\mu_{\text{H}}) = r \int_{-\infty}^{\infty} \frac{Z(E)}{1 + \exp\left(\frac{E - \mu_{\text{H}}}{RT}\right)} dE \quad (2)$$

with the maximum number r of available interstitial sites per metal atom. Kirchheim summarized several dependencies for the major defect types [2]. For a nanocrystalline material containing interstitial lattice sites with $Z(E) = \delta(E - E_0)$ as well as two additional trap sites ($i = 1, 2$) of Gaussian energy distribution (for example grain boundary and a further deep trap) gives [29]

$$Z(E) = (1 - f_1 - f_2)\delta(E - E_0) + \sum_{i=1}^2 \frac{f_i}{\sigma_i \sqrt{\pi}} \exp\left[-\left(\frac{E - E_i}{\sigma_i}\right)^2\right] \quad (3)$$

with the volume density f_i of the two additional trap sites. σ_i gives the widths of the Gaussian functions. These depend on the individual trap sites [18].

Fig. 3 visualizes the sensitivity of the adjustment of the parameters of Eq. (3) to the measured EMF-curve, for a Pd thin film electrochemically charged with hydrogen. The EMF U is proportional the chemical potential according to $\mu_{\text{H}} = (U - U_0)F$, with a reference potential U_0 with respect to an electrochemical reference electrode, and Faradays constant $F = 96485 \text{ A s mol}^{-1}$. Note that stress contributions, related to the substrate have been subtracted in the EMF-curves [29]. Fig. 3a shows the EMF curve of the ideal Pd-H system, following Sieverts law in the α -phase region up to its solubility limit x_{∞}^{max} . For the 80 nm thin Pd film Fig. 3b, the measured dependency strongly deviates from Sieverts law (straight red line). The contributions of interstitial sites E_0 , deep traps E_2 (Fig. 3c) and grain boundaries E_1 (Fig. 3d) are subsequently added to the fit curve. Fig. 3d containing all three contributions finally gives a satisfying fit to the measured data. The trap energy gives the position of shift in the chemical potential, the magnitude of the contribution relates to the density of the trap.

Tab. 1 summarizes the trap energies measured for different types of Pd material. Strong differences can be seen in the interstitial site energy of the matrix, as well as in the trap energies. The energies slightly depend on the type of material.

Table 1. Hydrogen binding energies in different traps, as measured in Pd materials.

Traps	Binding energy [kJ/mol]	Material	Reference
Matrix	4.7	Pd sheet	Wang [88]
	7.7		Wicke and Brodowsky [32]
	3.9	n-Pd	Mütschele and Kirchheim [18, 19]
Grain boundaries	4.8(3)	Pd film on V coated Sapphire substrate	Wagner and Pundt [29, 33]
	9.2	n-Pd	Mütschele and Kirchheim [18, 19]
Surface/interface sites: deep traps	0.5(1)	Pd film on Sapphire substrate	Wagner and Pundt [29]
	-42 (1)	Pd film on Sapphire substrate	Wagner and Pundt [29]

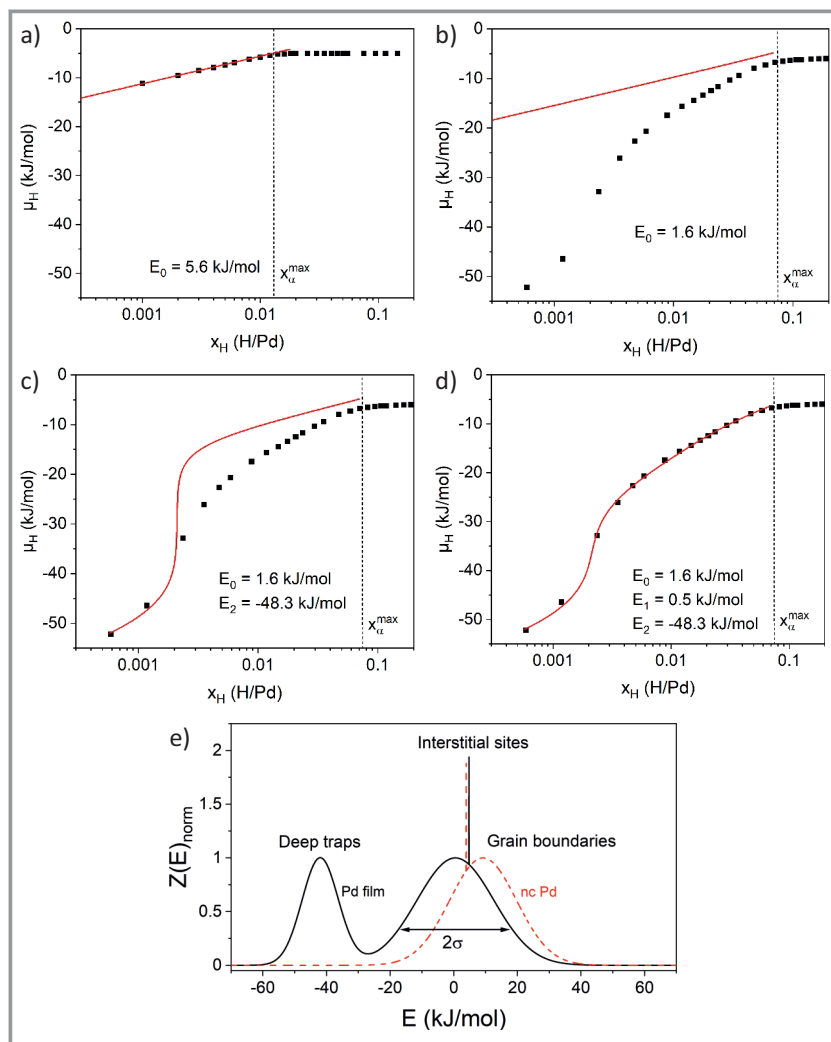


Figure 3. Measured chemical potentials in the solid solution Pd–H phase of a) bulk and b)–d) an 80 nm thin film on a Silicon substrate, up to the solubility limit $x_{\text{H}}^{\text{max}}$. While Sieverts line properly describes the bulk material in a), further microstructural defects have to be considered for the thin film. Successive addition of interstitial sites (b), deep traps (c), and grain boundaries (d) allows to properly fit the measured data via Eq. (2). e) gives the normalized derived density of the different site energies distribution $Z(E)$ in the Pd-film (black line, see also [3]) and, for comparison, the $Z(E)$ evaluated by Mütschle et al. for a nano-crystalline Pd material (nc Pd, red dotted line, see also [31]). The site energy distributions were normalized to the peak maxima for better visualization of the different site contributions.

Strong hydrogen bonding appears at surfaces or interfaces, the so-called deep traps, with binding energies of more than -40 kJ mol $^{-1}$. Grain boundaries offer low energy sites as well as high energy sites, the Gaussian distribution of site energies is rather broad. The mean value can be even higher than that of the interstitial sites. Adding deep traps such as interfaces between carbides and the metal can bind internal hydrogen and protect the metal from hydrogen embrittlement [34–37] – as long as there is no external hydrogen source.

hydrogen diffusion, especially in the bcc lattice structure. The temperature dependency of the diffusion coefficient D_i for interstitial diffusion is given by [38]

$$D_i = \frac{1}{6} d_{\text{O/T}}^2 n_{\text{O/T}} f \exp\left(\frac{\Delta S_{i,m}}{R}\right) \exp\left(-\frac{\Delta H_{i,m}}{RT}\right) = D_{0,i} \exp\left(-\frac{\Delta H_{i,m}}{RT}\right) \quad (4)$$

with the jump frequency f , approximated by the Debye frequency $f_D = 10^{13}$ s $^{-1}$ of the lattice vibrations, [38] the entropy for interstitial migration $\Delta S_{i,m}$ and the gas constant

6 Hydrogen Diffusion and Tunnelling Effects

In the solid solution basic metal structures, hydrogen occupies the interstitial sites of the lattice. Diffusion in the interstitial sites is by orders of magnitudes faster than substitutional diffusion in the lattice, as vacancy formation is not required. [38] The prominent interstitial sites have a tetrahedral (T) or an octahedral (O) arrangement of the adjacent metal atoms. The size of the interstitial sites scales with the size of the atoms, considered as spheres with a radius r_M . Thus, from strain energy arguments solely, hydrogen solution in interstitial sites is more favourable for metals built of large atoms.

In the fcc and the hcp lattice, the radius $r_{\text{O/T}}$ of the interstitial sizes, also considered as spheres, is $r_{\text{O}} = 0,414 r_M$, or $r_{\text{T}} = 0,225 r_M$, with a coordination number of the next nearest interstitial sites of the same type being $n_{\text{O}} = 12$ or $n_{\text{T}} = 6$, respectively. For the bcc lattice, $r_{\text{O}} = 0,155 r_M$, or $r_{\text{T}} = 0,291 r_M$, with $n_{\text{O}} = 4$ or $n_{\text{T}} = 4$. The number of O-sites and T-sites per atom is 3 and 6 for the bcc lattice, and 1 and 2 for the fcc or hcp lattice. The distance between the nearest neighbour O- and T-sites in the bcc lattice ($d_{\text{O}} = a/2$, $d_{\text{T}} = a/4$) is significantly smaller than that in the fcc or hcp structures ($d_{\text{O}} = a/\sqrt{2}$, $d_{\text{T}} = \sqrt{3}a/2$). Typical distances in bcc of $d_{\text{O}} = 1.4$ Å, and in fcc of $d_{\text{O}} = 2.7$ Å occur. This jump distance quadratically influences the diffusion coefficient D_i . But the enthalpy barrier $\Delta H_{i,m}$ between the nearest neighbour sites is much smaller for the bcc lattice, as there is no metal atom in the diffusion path. [1] This allows for an exponential increase of D_i and, finally, a very fast

$R = 8.314 \text{ J mol}^{-1} \text{ K}^{-1}$. An example for the structural influence on the diffusion coefficient is shown in Fig. 4, where the measured hydrogen diffusion coefficient is plotted for $\text{Pd}_{0.47}\text{Cu}_{0.53}$, in logarithmic scale as a function of the inverse temperature T (Arrhenius plot). [39] The Pd–Cu lattice structure is fcc for the whole concentration range, but offers a bcc B2 ordered intermetallic phase at low temperatures. Thus, both structures are available at around 47 at % Cu, as by quenching the fcc-phase can be kinetically conserved. The magnitude of D is strongly determined by the lattice structure. [4] At 0°C (upper axis), the diffusion coefficient of hydrogen in the fcc structure is about 4 orders of magnitude lower than in the bcc structure. The different slope reflects the different enthalpy barrier $\Delta H_{i,m}$.

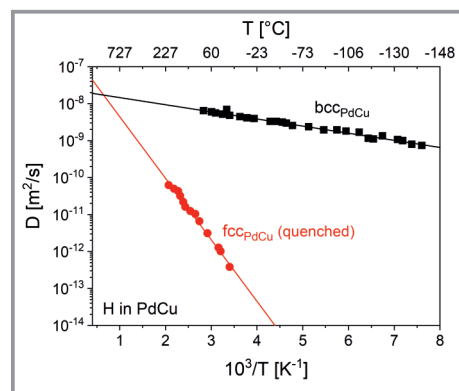


Figure 4. Measured hydrogen diffusion coefficient for $\text{Pd}_{0.47}\text{Cu}_{0.53}$, in stable bcc and metastable fcc lattice structures. The B2 (CsCl-structure type) ordered intermetallic phase occurs at low T in the middle of the concentration range. A strong influence of the structure on D is observed. Adapted from [39].

This structural dependency is of special importance for metals exposed to mechanical strain. For steels, if the austenite stability is insufficient, strain-induced martensite of bcc-like structure can form and affect the materials mechanical properties.

It should be also considered that hydrogen can propagate by the quantum mechanical tunnelling mechanism. This is of special importance for bcc metals such as V, Nb or Fe. For Nb, hydrogen tunnelling effects are already observed below about -50°C , by increased mobility compared to the expectations from the Arrhenius dependency. Consequently, strong differences between the hydrogen isotopes occur. For the bcc structure it is impossible to “freeze” hydrogen on an interstitial site. [40] This has to be considered in measurements to determine local hydrogen concentrations in metals, like secondary ion mass spectrometry (SIMS) or atom probe tomography (APT), where surface atoms are removed and, thus, always empty surface sites are offered for hydrogen to be trapped. [41] Accordingly, tunnelling effects are less pronounced for fcc lattices. [9]

Defects offer sites with different energies and different diffusion barriers, leading to hydrogen trapping. Since trap-

ping depends on the temperature, one always has to consider the temperature of operation and the relevant time frame, if one differentiates between diffusible hydrogen and non-diffusible hydrogen. While hydrogen might appear trapped and non-diffusible at low temperatures, it may be desorbed and diffusible at elevated temperatures. Under cyclic load, during material creep or at a propagating crack tip, when defects propagate with a certain velocity, the mobility of hydrogen becomes relevant for the hydrogen defect interaction, and also for the material properties. Depending on the velocity interplay between the defect and hydrogen, hydrogen can follow the defect or the defect escapes from hydrogen. Hence, hydrogen may affect the defect properties just as long as it remains located at the defect.

7 Defect Energies Affected by Hydrogen

Kirchheim developed a concept (DEFect ACTing AgeNTS) considering the change of defect energies γ by the presence of solutes, here hydrogen, [42] with Eq. (5) for constant volume, temperature, metal atom number and defect density ρ (given by the grain boundary area, the dislocation length or the number of vacancies per volume V).

$$\left. \frac{\partial \gamma}{\partial \mu_{\text{H}}} \right|_{T, V, n_{\text{M}}, \rho} = -\Gamma_{\text{H}} \quad (5)$$

The surplus amount of hydrogen located at the defect is called excess Γ_{H} . For small chemical potentials, hydrogen is not allocated at the defect. Therefore, the defect energy $\gamma = \gamma_0$ remains constant, as shown in Fig. 5. When the chemical potential reaches the site energy of the defect E_{d} , the excess increases and the defect energy γ gets smaller, according to Eq. (5). The change of the decay depends on the excess hydrogen. A constant maximum excess leads to a line with constant slope (line 1) which intercepts the abscissa at $\mu_{\gamma, \text{H}}$. If the excess steadily increases, the drop occurs faster (line 2). If a new H-rich phase is formed at the defect, the excess Γ_{H} and γ remain constant despite increasing concentration in the sample (line 3).

As the defect energy γ changes negatively with the excess Γ_{H} , hydrogen segregation results in a lowering of the defect energy. Hence, the amount of defects can increase in a material containing hydrogen. This has been shown in different materials and for different types of defects. For α -Nb-H, vacancy concentrations of $3 \cdot 10^{-5}$ have been detected in presence of 0.02 H/Nb, whereas the equilibrium concentration of thermal vacancies in Nb without hydrogen is negligible. [17] Under high chemical potentials (H_2 gas pressures of 5 GPa) and high temperatures of 700 – 800°C), Fukai and Okuma reported on superabundant vacancy concentrations of $1.8 \cdot 10^{-1}$ for Pd. [44]

The concept can explain the easier nucleation of dislocations by a reduction of the formation energy of dislocation.

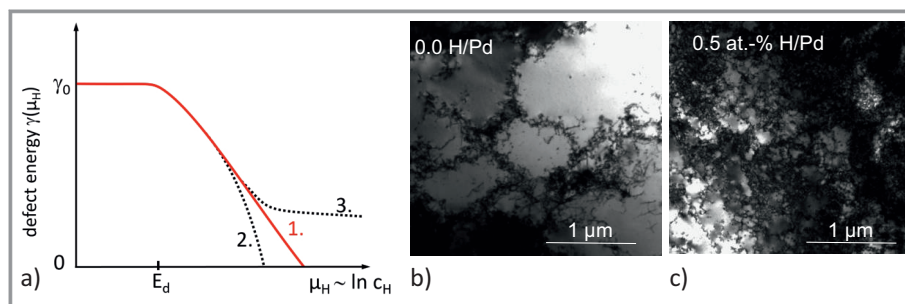


Figure 5. a) Development of the defect energy $\gamma(\mu_H)$ on the excess Γ_H . For low chemical potentials, there is no hydrogen located at defects and $\gamma = \gamma_0$. As μ_H approaches the defect energy E_d , γ decreases according to Eq. (5). The decrease depends on the excess Γ_H . For constant excess, $\gamma(\mu_H)$ linearly decreases (1), it decays faster for increasing excess (2) and it stays constant for the formation of a H-rich phase. A low $\gamma(\mu_H)$ allows for high defect densities. b) TEM micrograph of cold rolled Pd with reduction in thickness by 50 %, and c) charged with 0.005 H/Pd prior to rolling. The dislocation density is significantly increased (micrographs from Deutges, see also [43, 49, 52]).

Nanoindentation experiments support this effect by a reduced pop-in load in hydrogen containing metals. [45–48] It can also explain a faster dislocation mobility in hydrogen containing metals by the reduction of the formation energy of kink pairs. Increased dislocation densities were observed for example in Pd cold-rolled in the presence of hydrogen, [49, 50] or in Fe. [51] A decreased energy of dislocation formation has been observed by a reduced pop-in load during nanoindentation in H-loaded V by Deutges [52] or Tal-Gutelmacher et al. [53], in a H-loaded ferritic alloy by Gaspard et al. [54] or in deuterium plasma exposed W by Fang et al. [55].

It is assumed that the different models suggested for hydrogen embrittlement (it is noted that the wording ‘hydrogen embrittlement’ is misleading: hydrogen-induced failure can either happen via a brittle fracture but also via ductile fracture) such as hydrogen enhanced decohesion (HEDE), e.g., [56–58], adsorption-induced dislocation emission (AIDE), e.g., [59, 60], hydrogen-enhanced localized plasticity (HELP), e.g., [61–63], or hydrogen-enhanced strain-induced vacancies (HESIV), e.g., [64, 65], might be explained by this underlying thermodynamical concept. The change of the defect energy might also explain changes from ductile to brittle hydrogen effect behaviour, as above a certain excess hydrogen the defect energies can be even close to zero (line 1 and 2 in Fig. 5). This was calculated recently for hydrogen decorated pores along Ni (111) planes when hydrogen pressures exceed 100 MPa. According to the calculation, above this pressure, separation of (111) lattice planes can occur without applied external forces. [66]

8 Hydrogen Permeation

The hydrogen flux permeating through a material depends on the hydrogens diffusivity D_i and solubility x_H . Thus, the permeability P_H is given by the product of both quantities, [67]

$$P_H = x_H D_i = S_{0,i} \exp\left(\frac{\Delta H_\alpha}{RT}\right) D_{0,i} \exp\left(-\frac{\Delta H_{i,m}}{RT}\right) \quad (6)$$

This equation considers hydrogen permeation in the solid solution and contains Sieverts’ law, Eq. (1). P_H thereby exponentially depends on the enthalpy of hydrogen solution ΔH_α in the metal, and on the barrier for interstitial hydrogen diffusion $\Delta H_{i,m}$.

This general treatment considering the bulk quantities neglects any surface effects. It assumes perfect dissociative chemisorption of the hydrogen molecule

and no hydrogen traps at the surface. But according to Sect. 4, traps occur especially at the surface and change the local hydrogen content. However, the surface can be covered by other elements, or even coated with an additional layer. Gradients in the chemical potential, in the simplest case given by gradients in the hydrogen concentration, drive the permeation flux. Therefore, the surface conditions have to be considered as they influence the hydrogen permeation. [68]

Low hydrogen permeation coatings can be used as hydrogen barriers, to protect the material from external hydrogen. Rönnebroe et al. recently reviewed the actual hydrogen barrier coatings like oxides, nitrides, carbon, carbides, MAX-phases (layered, hexagonal carbides and nitrides, with M being an early transition metal, A being an A-group element and X being either carbon and/or nitrogen) and metals. [67] Most of the recent work focusses on ceramic-based barrier coatings.

High permeation membranes are used for hydrogen separation and purification, as long as just hydrogen is allowed to permeate through the metal in large quantity. This relates to its high diffusivity and solubility, when compared to other interstitial elements (e.g., O, N, C). Many membranes base of Pd-alloys, such as Pd–Ag. [69] Non-Pd-based alloy membranes usually are covered with protective Pd coating layers to prevent oxidation. [70] Nb, V, and Ta-based alloy membranes are less expensive and exhibit higher hydrogen permeability than Pd. However, they suffer from hydrogen embrittlement above a certain hydrogen content, called “ductile-to-brittle transition hydrogen concentration (DBTC)” [71]. The membrane has to possess a strong resistance against hydrogen embrittlement to fulfil its purpose.

9 Coatings: Mechanical Stress Effects

If a coating layer absorbs a greater amount of hydrogen on the interstitial sites of the lattice, the related lattice expansion can result in additional mechanical stress. [4, 72] For Nb- or Pd-layers adhered to Sapphire or Silicon substrates this was intensively studied for different microstructures and coating layer thicknesses. [73–78] Compressive mechanical stress ranging up to -8 GPa was measured in ultra-thin Nb layers of about 5 nm thickness, see Fig. 6a). [79] This stress results from the prevented lattice expansion in the adhered plane directions. For the case of rigid substrates linear elastic theory gives a stress of -8.9 GPa for 1 H/Nb in the considered orientation of the film. [4, 74, 79] In the film vertical direction, the film is mainly free to expand. Here the film expands strongly, because of the Poisson-effect.

Conventionally, high mechanical stress can be released by the system via plastic deformation, grain sliding or twinning or by detachment of the film from the substrate (buckling). [80] An optical micrograph of a detached film is presented in Fig. 6b). [81] It was recently shown that hydrogen-induced plastic deformation in the film can be partially suppressed when the coating layer thickness is thinner than about 40 nm. For coating layers below 8 nm thickness, plastic deformation is completely suppressed. [33, 82] These coatings suffer from ultra-high stress when they stay adhered. This high stress can strongly change the phase diagram. For the Nb-H system the miscibility gap between the α -phase and the hydride phase even vanishes, for temperatures above room temperature. [74] This experimental finding has been described by adding a stress related term $\Delta\mu_{ii}(\sigma_{ii}) = -v_0\eta_H\sigma_{ii}(x_H)$, containing the sum of the axial stresses $\sigma_{ii}(x_H)$, to the conventional equation (see for example [1]) for the chemical potential [29, 82]:

$$\mu_H = RT \ln \left(\frac{x_H}{r - x_H} \right) + E_0 - E_{HH}x_H - v_0\eta_H\sigma_{ii}(x_H) \quad (7)$$

with the maximum number of available sites per metal atom that can be occupied by hydrogen, the isotropic and linear hydrogen induced dilation factor $\eta_H = 1/(3x_H) \cdot \Delta V/V$ of the metal lattice and the molar volume of the interstitial sites v_0 . For the O-sites in Pd $v_0 = 8.56 \cdot 10^{-6} \text{ m}^3 \text{ mol}^{-1}$ [32]. For T-sites in Nb the molar volume of available sites is $v_T = 9.29 \cdot 10^{-6} \text{ m}^3 \text{ mol}^{-1}$ [74, 83]. In the latter case it has to be taken into account that not all tetrahedral interstitial sites can be occupied by hydrogen according to Switendicks criterion, requiring a minimum H–H distance of 2.1 \AA . [84]

This additional stress term destabilizes the hydride phase and hence can increase the solubility limit of the α -phase. Thus, it protects the film from unwanted hydride formation. Hydride formation also can trigger hydrogen embrittlement. On top of that, coating detachment does not easily happen when the coating is ultra-thin: The elastic energy stored in the thin film does not suffice to nucleate and open a detaching crack. [85] Thus, for membranes an ideal thick-

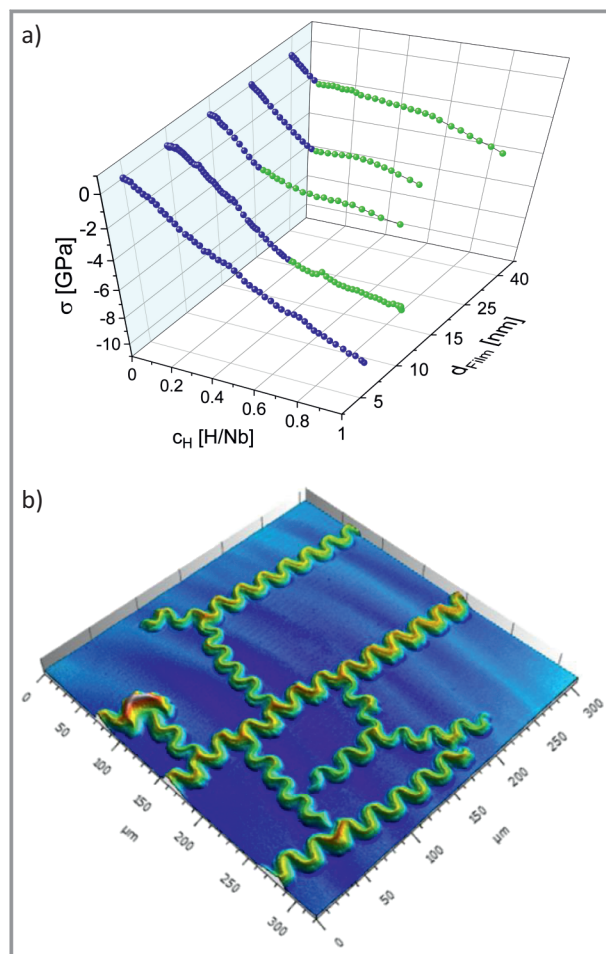


Figure 6. a) Mechanical stress measured via substrate curvature for different hydrogen concentrations in Nb films (5–40 nm) on Sapphire, capped with a Pd layer. The blue dots represent linear elastic stress increase, the green dots represent plastic deformation. For very thin films purely elastic stress development is measured, reaching -8.3 GPa. All films stay adhered to the substrate. [86] b) Detachment pattern observed by confocal microscopy on a Nb film (200 nm) on Sapphire substrate, with a cap and a bottom layer of Pd. The greenish regions (buckles) are detached from the substrate and lifted by about $1.5 \mu\text{m}$ above the base level (blue color). [87]

ness has to be found, to safely protect the membrane material from oxidation and to allow for high hydrogen flux.

Conclusion

The interaction of hydrogen with metals is manifold and many different aspects have to be considered, when the proper materials are planned to be chosen for a special application of hydrogen. This targets hydrogen gas stored in a container made out of a structural material, hydrogen atoms stored in a metal or material lattice, or hydrogen transport through membranes or in infrastructure components. Some basic aspects have been presented in this man-

uscript. Many studies of researchers worldwide on many different materials offer deep insights into the topic. A large quantity of background information is already at hand and supports us in a safe and sustainable application of hydrogen as a future energy carrier for renewable energy.

Acknowledgment

The authors like to thank the Deutsche Forschungsgemeinschaft for continuous support of their research. Open access funding enabled and organized by Projekt DEAL.



Astrid Pundt received her diploma in Physics at the Technical University of Braunschweig and graduated at Göttingen University in Metal Physics. She received the apl. Professorship in Physics at Göttingen University in 2009. In 2010 she visited Uppsala University in Sweden for lectures and research. Since 2018,

she works as full professor at the Karlsruhe Institute of Technology KIT, as director of the Institute of Applied Materials – Materials Engineering (IAM-WK). The research focus is on hydrogen in contact with many different types of materials, used for energy storage or as structural material in hydrogen environment, protective coatings and materials for fuel cells or electrolyzers.



Stefan Wagner is group leader of the “defects in materials” team at the IAM-WK at KIT. He studied physics at the University of Göttingen, where he received his PhD in the field of “Palladium-hydrogen thin films as a model system” in 2014 in the research group of Prof. Astrid Pundt. His research focuses on the thermodynamics of

metal-hydrogen systems, that serve as role models to study alloy thermodynamics with microstructural and elastic constraints. The gained knowledge is applied to the optimization of solid-state hydrogen storage systems and the understanding of the hydrogen embrittlement phenomena in nanostructured metals.

References

- [1] Y. Fukai, *The Metal-Hydrogen System : Basic Bulk Properties*, Springer Series in Materials Science, Vol. 21, Springer, Berlin **2005**. DOI: <https://doi.org/10.1007/3-540-28883-X>
- [2] H. Vehoff, *Hydrogen in Metals III*, Topics in Applied Physics, Vol. 73, Springer, Berlin **1997**, 215–278. DOI: <https://doi.org/10.1007/BFb0103398>
- [3] L. Schlapbach, *Hydrogen in Intermetallic Compounds II*, Topics in Applied Physics, Vol. 67, Springer, Berlin **2005**, 15–95.
- [4] A. Pundt, R. Kirchheim, *Annu. Rev. Mater. Res.* **2006**, *36*, 555–608. DOI: <https://doi.org/10.1146/annurev.matsci.36.090804.094451>
- [5] H. Conrad, G. Ertl, E. E. Latta, *Surf. Sci.* **1974**, *41* (2), 435–446. DOI: [https://doi.org/10.1016/0039-6028\(74\)90060-0](https://doi.org/10.1016/0039-6028(74)90060-0)
- [6] R. J. Behm, K. Christmann, G. Ertl, *Surf. Sci.* **1980**, *99* (2), 320–340. DOI: [https://doi.org/10.1016/0039-6028\(80\)90396-9](https://doi.org/10.1016/0039-6028(80)90396-9)
- [7] E. Wendler-Kalsch, *Wasserst. Korros.* **2000**, *2*, 7–53.
- [8] B. Isecke, *Korrosion im Bauwesen*, Deutscher Verband für Materialprüfung e. V., Berlin **1986**, 79–103.
- [9] G. A. Lange, M. Pohl, *Systematische Beurteilung Technischer Schadensfälle*, Wiley-VCH, Weinheim **2014**.
- [10] *Hydrogen as a Future Energy Carrier* (Eds: A. Züttel, A. Borgschulte, L. Schlapbach), Wiley-VCH, Weinheim **2008**.
- [11] L. Schlapbach, A. Züttel, *Nature* **2001**, *414* (6861), 353–358. DOI: <https://doi.org/10.1038/35104634>
- [12] R. Griessen, I. A. M. E. Giebels, B. Dam, *Optical properties of metal-hydrides: switchable mirrors*, Vrije Universiteit Amsterdam **2004**.
- [13] L. Schlapbach, J. P. Burger, J. E. Bonnet, P. Thiry, Y. Petroff, *Surf. Sci.* **1987**, *189–190*, 747–750. DOI: [https://doi.org/10.1016/S0039-6028\(87\)80509-5](https://doi.org/10.1016/S0039-6028(87)80509-5)
- [14] E. Eyring, K. A. Gschneidner, *Handbook of the Chemistry and Physics of the Rare Earth*, Elsevier, Amsterdam **1995**.
- [15] J. N. Huiberts, R. Griessen, J. H. Rector, R. J. Wijngaarden, J. P. Dekker, D. G. de Groot, N. J. Koeman, *Nature* **1996**, *380* (6571), 231–234. DOI: <https://doi.org/10.1038/380231a0>
- [16] G. Alefeld, J. Volkl, *Hydrogen in Metals: Application-oriented properties*, Springer, Berlin **1978**. DOI: <https://doi.org/10.1007/3-540-08883-0>
- [17] J. Čížek, I. Procházka, F. Bečvář, R. Kužel, M. Cieslar, G. Brauer, W. Anwand, R. Kirchheim, A. Pundt, *Phys. Rev. B* **2004**, *69* (22), 224106. DOI: <https://doi.org/10.1103/physrevb.69.224106>
- [18] T. Mütschele, R. Kirchheim, *Scr. Metall.* **1987**, *21* (2), 135–140. DOI: [https://doi.org/10.1016/0036-9748\(87\)90423-6](https://doi.org/10.1016/0036-9748(87)90423-6)
- [19] T. Mütschele, R. Kirchheim, *Scr. Metall.* **1987**, *21* (8), 1101–1104. DOI: [https://doi.org/10.1016/0036-9748\(87\)90258-4](https://doi.org/10.1016/0036-9748(87)90258-4)
- [20] M. Maxelon, A. Pundt, W. Pyckhout-Hintzen, R. Kirchheim, *Scr. Mater.* **2001**, *44* (5), 817–822. DOI: [https://doi.org/10.1016/S1359-6462\(00\)00654-0](https://doi.org/10.1016/S1359-6462(00)00654-0)
- [21] M. Maxelon, A. Pundt, W. Pyckhout-Hintzen, J. Barker, R. Kirchheim, *Acta Mater.* **2001**, *49* (14), 2625–2634. DOI: [https://doi.org/10.1016/s1359-6454\(01\)00185-9](https://doi.org/10.1016/s1359-6454(01)00185-9)
- [22] K. Christmann, *Surf. Sci. Rep.* **1988**, *9* (1–3), 1–163. DOI: [https://doi.org/10.1016/0167-5729\(88\)90009-X](https://doi.org/10.1016/0167-5729(88)90009-X)
- [23] R. J. Behm, K. Christmann, G. Ertl, *Surf. Sci.* **1980**, *99* (2), 320–340. DOI: [https://doi.org/10.1016/0039-6028\(80\)90396-9](https://doi.org/10.1016/0039-6028(80)90396-9)
- [24] A. Pundt, *Adv. Eng. Mater.* **2004**, *6*, 11–21. DOI: <https://doi.org/10.1002/adem.200300557>
- [25] A. M. De Jong, J. W. Niemantsverdriet, *Surf. Sci.* **1990**, *233* (3), 355–365. DOI: [https://doi.org/10.1016/0039-6028\(90\)90649-S](https://doi.org/10.1016/0039-6028(90)90649-S)
- [26] N. Boes, H. Züchner, *J. Less-Common Met.* **1976**, *49*, 223–240. DOI: [https://doi.org/10.1016/0022-5088\(76\)90037-0](https://doi.org/10.1016/0022-5088(76)90037-0)

- [27] R. Kirchheim, *Acta Metall.* **1981**, 29 (5), 845–853. DOI: [https://doi.org/10.1016/0001-6160\(81\)90127-9](https://doi.org/10.1016/0001-6160(81)90127-9)
- [28] R. Kirchheim, *Prog. Mater. Sci.* **1988**, 32 (4), 261–325. DOI: [https://doi.org/10.1016/0079-6425\(88\)90010-2](https://doi.org/10.1016/0079-6425(88)90010-2)
- [29] S. Wagner, A. Pundt, *AIMS Mater. Sci.* **2020**, 7 (4), 399–419. DOI: <https://doi.org/10.3934/mat.2020.4.399>
- [30] R. Kirchheim, *Solid solutions of hydrogen in complex materials*, Solid State Physics, Vol. 59, Elsevier, Amsterdam **2004**, 203–291. DOI: [https://doi.org/10.1016/S0081-1947\(04\)80004-3](https://doi.org/10.1016/S0081-1947(04)80004-3)
- [31] R. Kirchheim, T. Mütschele, W. Kieninger, H. Gleiter, R. Birringer, T. D. Koble, *Mater. Sci. Eng.* **1988**, 99 (1–2), 457–462. DOI: [https://doi.org/10.1016/0025-5416\(88\)90377-1](https://doi.org/10.1016/0025-5416(88)90377-1)
- [32] E. Wicke, H. Brodowsky, H. Züchner, *Hydrogen in palladium and palladium alloys*, Topics in Applied Physics, Vol. 29, Springer, Berlin **1978**. DOI: https://doi.org/10.1007/3-540-08883-0_19
- [33] S. Wagner, A. Pundt, *Acta Mater.* **2011**, 59 (5), 1862–1870. DOI: <https://doi.org/10.1016/j.actamat.2010.11.052>
- [34] Q. Xu, J. Zhang, *Sci. Rep.* **2017**, 7 (1), 16927. DOI: <https://doi.org/10.1038/s41598-017-17263-8>
- [35] J. Lee, T. Lee, D.-J. Mun, C. M. Bae, C. S. Lee, *Sci. Rep.* **2019**, 9 (1), 5219. DOI: <https://doi.org/10.1038/s41598-019-41436-2>
- [36] L. B. Peral, I. Fernández-Pariente, C. Colombo, C. Rodríguez, J. Belzunce, *Materials* **2021**, 14 (23), 7269. DOI: <https://doi.org/10.3390/ma14237269>
- [37] D. Di Stefano, R. Nazarov, T. Hickel, J. Neugebauer, M. Mrovec, C. Elsässer, *Phys. Rev. B* **2016**, 93 (18), 184108. DOI: <https://link.aps.org/doi/10.1103/PhysRevB.93.184108>
- [38] G. Gottstein, *Physical Foundations of Materials Science*, Springer, Berlin **2004**. DOI: <https://doi.org/10.1007/978-3-662-09291-0>
- [39] Y. Fukai, H. Sugimoto, *Adv. Phys.* **1985**, 34 (2), 263–326.
- [40] P. Kesten, A. Pundt, G. Schmitz, M. Weisheit, H. U. Krebs, R. Kirchheim, *J. Alloys Compd.* **2002**, 330, 225–228. DOI: [https://doi.org/10.1016/S0925-8388\(01\)01596-1](https://doi.org/10.1016/S0925-8388(01)01596-1)
- [41] M. Wilke, G. Teichert, R. Gemma, A. Pundt, R. Kirchheim, H. Romanus, P. Schaaf, *Thin Solid Films* **2011**, 520 (5), 1660–1667. DOI: <https://doi.org/10.1016/j.tsf.2011.07.058>
- [42] R. Kirchheim, *Int. J. Mater. Res.* **2009**, 100 (4), 483–487. DOI: <https://doi.org/10.3139/146.110065>
- [43] Y. Z. Chen, H. P. Barth, M. Deutges, C. Borchers, F. Liu, R. Kirchheim, *Scr. Mater.* **2013**, 68 (9), 743–746. DOI: <https://doi.org/10.1016/j.scriptamat.2013.01.005>
- [44] Y. Fukai, N. Okuma, *Phys. Rev. Lett.* **1994**, 73 (12), 1640–1643. DOI: <https://doi.org/10.1103/PhysRevLett.73.1640>
- [45] D. Wang, X. Lu, Y. Deng, X. Guo, A. Barnoush, *Acta Mater.* **2019**, 166, 618–629. DOI: <https://doi.org/10.1016/j.actamat.2018.12.055>
- [46] A. Barnoush, H. Vehoff, *Acta Mater.* **2010**, 58 (16), 5274–5285.
- [47] A. Barnoush, H. Vehoff, *Scr. Mater.* **2006**, 55 (2), 195–198. DOI: <https://doi.org/10.1016/j.scriptamat.2006.03.041>
- [48] G. Stenerud, R. Johnsen, J. S. Olsen, J. He, A. Barnoush, *Int. J. Hydrogen Energy* **2017**, 42 (24), 15933–15942.
- [49] M. Deutges, H. P. Barth, Y. Chen, C. Borchers, R. Kirchheim, *Acta Mater.* **2015**, 82, 266–274.
- [50] Y. Z. Chen, H. P. Barth, M. Deutges, C. Borchers, F. Liu, R. Kirchheim, *Scr. Mater.* **2013**, 68 (9), 743–746. DOI: <https://doi.org/10.1016/j.scriptamat.2013.01.005>
- [51] Y. Sugiyama, K. Takai, *Acta Mater.* **2021**, 208, 116663. DOI: <https://doi.org/10.1016/j.actamat.2021.116663>
- [52] M. Deutges, *Einfluss von gelöstem Wasserstoff auf die Versetzungsbildung bei plastischer Verformung von Metallen*, Ph.D. Thesis, Georg-August-Universität Göttingen **2016**. DOI: <https://doi.org/10.53846/goediss-5556>
- [53] E. Tal-Gutelmacher, R. Gemma, C. A. Volkert, R. Kirchheim, *Scr. Mater.* **2010**, 63 (10), 1032–1035. DOI: <https://doi.org/10.1016/j.scriptamat.2010.07.039>
- [54] V. Gaspard, G. Kermouche, D. Delafosse, A. Barnoush, *Mater. Sci. Eng. A* **2014**, 604, 86–91. DOI: <https://doi.org/10.1016/j.msea.2014.02.041>
- [55] X. Fang, A. Kreter, M. Rasinski, C. Kirchlechner, S. Brinckmann, C. Linsmeier, G. Dehm, *J. Mater. Res.* **2018**, 33 (20), 3530–3536. DOI: <https://doi.org/10.1557/jmr.2018.305>
- [56] A. R. Troiano, *Trans. ASME* **1960**, 52, 54–81.
- [57] R. A. Oriani, *Ber. Bunsengesellschaft Phys. Chem.* **1972**, 76 (8), 848–857. DOI: <https://doi.org/10.1002/bbpc.19720760864>
- [58] W. W. Gerberich, R. A. Oriani, M. J. Lji, X. Chen, T. Foecke, *Philos. Mag. A* **1991**, 63 (2), 363–376. DOI: <https://doi.org/10.1080/01418619108204854>
- [59] S. P. Lynch, *Acta Metall.* **1988**, 36 (10), 2639–2661. DOI: [https://doi.org/10.1016/0001-6160\(88\)90113-7](https://doi.org/10.1016/0001-6160(88)90113-7)
- [60] S. P. Lynch, *Metallography* **1989**, 23 (2), 147–171. DOI: [https://doi.org/10.1016/0026-0800\(89\)90016-5](https://doi.org/10.1016/0026-0800(89)90016-5)
- [61] C. D. Beachem, *Metall. Mater. Trans. B* **1972**, 3, 441–455. DOI: <https://doi.org/10.1007/BF02642048>
- [62] H. K. Birnbaum, P. Sofronis, *Mater. Sci. Eng. A* **1994**, 176 (1–2), 191–202. DOI: [https://doi.org/10.1016/0921-5093\(94\)90975-X](https://doi.org/10.1016/0921-5093(94)90975-X)
- [63] H. K. Birnbaum, I. M. Robertson, P. Sofronis, D. Teter, in *Proc. of the Second Int. Conf. on Corrosion-Deformation Interactions, CDF'96*, Maney Publishing, Leeds **1998**, 172–195.
- [64] K. Takai, H. Shoda, H. Suzuki, M. Nagumo, *Acta Mater.* **2008**, 56 (18), 5158–5167. DOI: <https://doi.org/10.1016/j.actamat.2008.06.031>
- [65] M. Nagumo, *ISIJ Int.* **2001**, 41 (6), 590–598. DOI: <https://doi.org/10.2355/isijinternational.41.590>
- [66] R. Kirchheim, B. Someday, P. Sofronis, *Acta Mater.* **2015**, 99, 87–98. DOI: <https://doi.org/10.1016/j.actamat.2015.07.057>
- [67] E. C. E. Rönnebro, R. L. Oelrich, R. O. Gates, *Molecules* **2022**, 27 (19), 6528. DOI: <https://doi.org/10.3390/molecules27196528>
- [68] E. Billeter, S. Kazaz, A. Borgschulte, *Adv. Mater. Interfaces* **2022**, 9 (23), 2200767. DOI: <https://doi.org/10.1002/admi.202200767>
- [69] A. G. Knapton, *Platinum Met. Rev.* **1977**, 21 (2), 44–50.
- [70] A. Suzuki, H. Yukawa, *Membranes* **2020**, 10 (6), 120. DOI: <https://doi.org/10.3390/membranes10060120>
- [71] Y. Matsumoto, H. Yukawa, T. Nambu, in *Proc. 2nd International Conference Small Sample Test Technics*, Ocelot, Prague **2012**.
- [72] R. Kirchheim, A. Pundt, in *Physical Metallurgy* (Eds: D. E. Laughlin, K. Hono), Elsevier, Amsterdam **2015**. DOI: <https://doi.org/10.1016/B978-0-444-53770-6.00025-3>
- [73] V. Burlaka, S. Wagner, M. Hamm, A. Pundt, *Thin Solid Films* **2019**, 679, 64–71. DOI: <https://doi.org/10.1016/j.tsf.2019.04.002>
- [74] S. Wagner, P. Klose, V. Burlaka, K. Nörthemann, M. Hamm, A. Pundt, *ChemPhysChem* **2019**, 20 (14), 1890–1904. DOI: <https://doi.org/10.1002/cphc.201900247>
- [75] V. Burlaka, K. Nörthemann, A. Pundt, *Nano Lett.* **2016**, 16, 6207. DOI: <https://doi.org/10.4028/www.scientific.net/DDF.371.160>
- [76] S. Wagner, A. Pundt, *Int. J. Hydrogen Energy* **2016**, 41, 2727. DOI: <https://doi.org/10.1016/j.ijhydene.2015.11.063>
- [77] V. Burlaka, S. Wagner, M. Hamm, A. Pundt, *Nano Lett.* **2016**, 16 (10), 6207–6212. DOI: <https://doi.org/10.1021/acs.nanolett.6b02467>
- [78] S. Wagner, T. Kramer, H. Uchida, P. Dobron, J. Cizek, A. Pundt, *Acta Mater.* **2016**, 114, 116–125. DOI: <https://doi.org/10.1016/j.actamat.2016.05.023>
- [79] M. Hamm, V. Burlaka, S. Wagner, A. Pundt, *Appl. Phys. Lett.* **2015**, 106 (24), 243108. DOI: <https://doi.org/10.1063/1.4922285>

- [80] A. Pundt, E. Nikitin, P. Pekarski, R. Kirchheim, *Acta Mater.* **2004**, *52*, 1579. DOI: <https://doi.org/10.1016/j.actamat.2003.12.003>
- [81] S. Wagner, A. Pundt, *Appl. Phys. Lett.* **2008**, *92*, 051914. DOI: <https://doi.org/10.1063/1.2841636>
- [82] S. Wagner, A. Pundt, *Int. J. Hydrogen Energy* **2016**, *41*, 2727. DOI: <https://doi.org/10.1016/j.ijhydene.2015.11.063>
- [83] S. Wagner, M. Moser, C. Greubel, K. Peeper, P. Reichart, A. Pundt, G. Dollinger, *Int. J. Hydrogen Energy* **2013**, *38*, 13822. DOI: <https://doi.org/10.1016/j.ijhydene.2013.08.006>
- [84] A. C. Switendick, *Z. Phys. Chem.* **1979**, *117*, 89–112. DOI: <https://doi.org/10.1524/zpch.1979.117.117.089>
- [85] A. Pundt, E. Nikitin, P. Pekarski, R. Kirchheim, *Acta Mater.* **2004**, *52*, 1579. DOI: <https://doi.org/10.1016/j.actamat.2003.12.003>
- [86] P. Klose, M. Hamm, V. Roddatis, A. Pundt, *Int. J. Hydrogen Energy* **2017**, *42*, 22583. DOI: <https://doi.org/10.1016/j.ijhydene.2017.04.229>
- [87] E. Mora, S. Wagner, A. Pundt, unpublished.
- [88] Wang, unpublished.

DOI: 10.1002/cite.202300235

Hydrogen Interactions with Defects in Materials

Astrid Pundt, Stefan Wagner*

Review Article: Basic properties of hydrogen in materials and some resulting consequences for the materials properties are addressed in a focussed manner to shortly introduce into the field. Hydrogen solution in materials, hydride formation, hydrogen mobility, the interaction of hydrogen with defects, also influenced by constraint conditions are shortly presented.

